Available online at www.sciencedirect.com

ScienceDirect

Procedia Manufacturing 38 (2019) 17–24

Procedia MANUFACTURING

www.elsevier.com/locate/procedia

29th International Conference on Flexible Automation and Intelligent Manufacturing (FAIM2019), June 24-28, 2019, Limerick, Ireland.

Additive manufacturing of PLA/HNT nanocomposites for biomedical applications

Chaitra Venkatesh[a], Evert Fuenmayor[a], Patrick Doran[a], Ian Major[a], John G Lyons[a], Declan M Devine[a]*

[a]*Athlone Institute of Technology, Dublin Road, Athlone, N37 HD68, Ireland*

Abstract

Additive manufacturing has been of great interest of research in various applications due to their ease in processability, cost effectiveness and adaptability. In this study Poly Lactic Acid (PLA) was used as the base polymer which was reinforced with Halloysite Nanotubes (HNT) powder as they are known to be biodegradable and has high mechanical properties individually.
HNT loadings with 3% and 5% were added to PLA by the method of twin screw extrusion and pelletized. For comparison, the PLA on its own was also extruded and pelletized. The resultant homogeneous pellets was extruded successfully into filaments of 1.75±0.10 mm diameter using twin screw extruder with specialized die fixed to the extruder for the manufacture of production grade 3D printing filament. This resultant filament was utilized for Fused Filament Fabrication (FFF) into standard tensile test bars and 25mm medical implants using a standard FFF printing machine.
The 3D printed samples were characterized for mechanical properties by uniaxial tensile test and thermal stability by Differential scanning calorimetry. Interestingly there was no significant change in the mechanical properties of the 3D printed tensile bars due to the processing parameters during FFF. However, the decrease in cold crystallization temperature by DSC indicates the nucleating effect of the HNT on the PLA matrix which in turn increases the mechanical properties. We could successfully 3D print model medical implants.

Keywords: Additive manufacturing; Fused Filament Fabrication; biodegradable stents; polylactic acid; halloysite nanotubes

* Corresponding author. Tel.: +353 (0)90 64 68291; fax: +0-000-000-0000 .
E-mail address: ddevine@ait.ie

10.1016/j.promfg.2020.01.003

1. Introduction

Additive manufacturing (AM) also known as three-dimensional (3D) printing has increase in research interest particularly in various medical applications due to its transformative nature and ability of customization. Recent research has explored the areas such as 3D printing of tablets for more precise controlled drug delivery, patient specific prostheses, tissue structures which are in the early stage of development for potential deployment in future [1].

One such area of interest is 3D printed implantable medical devices. Although the real application of 3D fabricated stents are limited because of material and machine constraints, much research is ongoing on in the areas such as 3D printed PLA/PCL cardiovascular stent [2], 3D printed ureteric stent [3], nasal stent [4] for potential future application. Fused Deposition Modeling (FDM) often referred as Fused Filament Fabrication (FFF) is one of the most widespread technology of extrusion based AM [5]. In this method, the thermoplastic filament is extruded on to a surface in X, Y and Z co-ordinates to fabricate a 3D structure as designed from as software and the process is controlled by the computer [6], [7]. Several studies have investigated various polymer nanocomposites for FFF [8]–[11].

Nanocomposites are emerging potentially in various industries due to excellent mechanical, electrical and thermal properties. The nanomaterial can be reinforced into the host matrices by 3D printing to produce nanocomposite signifies numerous advantages due to its properties and also improves the homogeneity of the product. [12] The high viscosity of the thermoplastics can be further increased by the addition of nanofillers which effects the printability of the nanocomposite filament. This can be addressed by opting for suitable mixing strategies while compounding to enhance dispersion of the nanomaterial into the polymer matrix. Various other methods such as solution mixing by sonication and high shear mixing by extrusion can be employed to reinforce the nanomaterial into the polymer matrix before 3D printing [13].

Nanocomposites have enormous potential in 3D printing applications. As shrinking the scale size to nanoscale can change the properties of the materials, a variety of nanomaterials such as carbon nanotubes, graphene, metal nanoparticles are used in 3D printing for various applications [14]. Several research has been conducted to study the physical properties of the final printed part when they are blended with nanomaterials. Recent studies show that in FFF the mechanical properties of the filament can be increased by addition of the nanofillers.

In this study we process the polymer PLA with a nanoclay HNT by the method of Hot Melt Extrusion (HME). The resultant PLA/HNT nanocomposite was pelletized and was extruded by HME to produce 3D printable filaments of diameter size 1.75±0.10 mm. These filaments were 3D printed by the method of FFF to make standard tensile bars for mechanical characterization and we aim to see if the PLA/HNT nanocomposite is 3D printable by varying the percentages of HNT nanoclay for comparison but keeping the 3D printing parameters the same for all the PLA and PLA/HNT nanocomposite samples. We also developed implants for medical applications by the method of which can potentially be adapted specifically for 3D printing of stents for various anatomical applications.

Nomenclature

AM	Additive manufacturing
FFF	Fused Filament Fabrication
HME	Hot melt Extrusion
HNT	Halloysite nanotubes
PLA	Poly Lactic Acid

2. Experimental Details

2.1. Materials

PLA was obtained from Corbion, PLA LX 175. The density of the PLA is 1.24 g/cm³. HNT was supplied by Applied Minerals; DRAGONITE-HP and has a density of 2.56 g/cm³. The PLA and HNT were dried in the oven at 80°C for 4 hours. The moisture content of the PLA was measured before processing for less than 100 ppm.

2.2. Methods

Compounding was performed by using APV (Model MP19TC (25:1)) (APV Baker, Newcastle-under-Lyme, UK) twin-screw compounder with 16 mm diameter screws. The temperature profile was maintained at (from feeder to the die) 190/180/170/170/160/140/120/50°C. The extrusion was performed at a screw speed of 140 rpm with the mass fractions of 100:0, 97:3 and 95:5 for PLA: HNT and are referred here as PLA, PLA/HNT3% and PLA/HNT5% respectively. The extrudate was drawn through a cooler belt and pelletized.

These pellets were reprocessed using the same machine into 3D printing filament of PLA and PLA/HNT. The metal die used for extrusion point had a bore diameter of 1.75 mm. The extrusion temperature was adjusted through a control panel and the melt temperature used for PLA pellets was 170 °C. This filament extrude was passed through cooler belt and finally wound onto a spool for 3D printing.

Once the filaments were extruded, they were printed into tensile test specimen and implant using a FFF 3D printer (MakerGear M2 3D printer, US). The nozzle temperature was fixed at 200°C, bed temperature at 70°C with 25% infill for all the filaments. The STL file generated from the designing of the implant and the tensile bars from SolidWorks software was used to dictate the construct dimensions to the printer through MakerGear.

Mechanical properties of the PLA/HNTs composites were characterized by tensile testing, which was carried out on a Lloyd Lr10k tensometer (Lloyd Instruments Ltd, West Sussex, UK) using a 2.5 kN load cell on ASTM standard test specimens at a strain rate of 10 mm/min (n = 5). Data was recorded using NexygenTM software. The tensile tests were carried out in adherence to ASTM D 882. Five test specimens were analyzed per group, and before testing, the thickness of each sample was measured. The percentage strain at maximum load, stress at maximum load, stiffness, and Young's Modulus of each sample was recorded.

DSC analysis was carried out in triplicate using a DSC 2920 Modulated DSC (TA Instruments, New Castle, DE, USA) with a nitrogen flow rate of 20ml/min to prevent oxidation. Calibration of the instrument was performed using indium as standard. Tests were conducted on samples weighing between 8 and 12 mg. Samples were measured on a Sartorius scales (MC 210 P), capable of being read to five decimal places. Samples were crimped in non-perforated aluminum pans, with an empty crimped aluminum pan used as the reference. The thermal history was removed by heating samples from 20°C to 220°C at the rate of 30°C/min and then held isothermally at 220°C for 10 min. The samples were cooled from 220°C to 20°C at 30°C/min. Finally, the thermal properties of the samples were recorded by heating the samples from 20°C to 220°C at the rate of 10°C/min, glass transition temperature, cold crystallization temperature and melting temperature of each sample were recorded.

3. Results

Virgin PLA and PLA/HNTs nanocomposites were melt compounded, pelletized and melt compounded to filaments at screw speeds of 140 rpm without difficulty. The extruded PLA filaments had small bubble like structures as shown in Fig 1. However, the PLA/HNTs nanocomposites filaments changed in color from transparent to opaque in particular the 5% nanocomposite. The resultant filaments of PLA and PLA/HNT nanocomposites had diameter size of 1.75±0.10 mm.

Fig. 1. Photographs of the filaments produced by twin screw extrusion (a) PLA (b) PLA/HNT 3% (c) PLA/HNT 5%.

The PLA and PLA/HNT nanocomposite filaments were used for 3D printing of tensile test bars. The morphology of the 3D printed samples was investigated using an optical microscope and a detail picture of a sample corner is reported in Fig 2. The 3D printing of tensile test bars of PLA was processed without difficulty. However, the 3D printing of the nanocomposites were difficult to process and the 3D printed bars had denser infill as the percentage of the HNT increased along with change in color as shown in Fig 2.

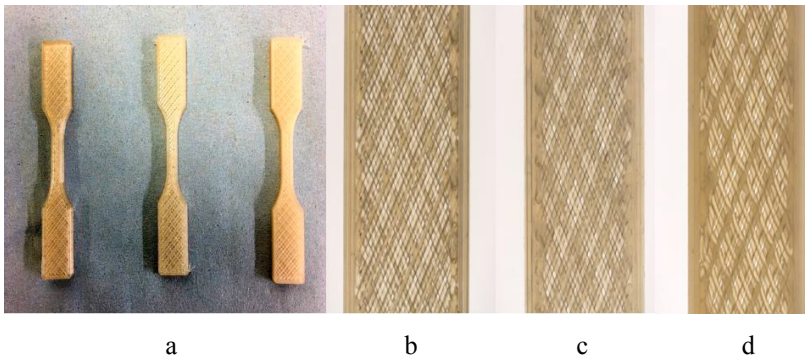

Fig. 2. Photographs from optical microscope of 3D printed tensile bars (a) (L-R) PLA, PLA/HNT 3% and PLA/HNT 5% nanocomposites. (b) Zoomed in photograph of PLA (c) zoomed in photograph of PLA/HNT 3% and (d) zoomed in photograph of PLA/HNT 5% nanocomposite indicates the infill pattern becomes denser with increase in the nanoclay percentage along with change in color.

The 3D printed tensile test bars were characterized for mechanical properties by uniaxial tensile testing and the tensile test results of PLA and PLA/HNT nanocomposite 3D printed tensile bars are as shown in Table 1.

Table 1. Mechanical properties of PLA and PLA/HNT nanocomposites

Batch	Young's Modulus	Stiffness	Tensile Strength	Elongation at break
PLA	391.22±32.02	240.61±19.86	33.37±1.9	14.71±4.52
PLA/HNT3%	443.58±41.11	269.11±12.22	37.44±5.11	14.7±2.55
PLA/HNT5%	357.10±69.24	224.3±43.49	29.97±4.54	12.75±0.31

The mechanical properties did not show any significant difference between the PLA and PLA/HNT nanocomposites 3D printed tensile samples. This result is in contrast with other research work and our previous research which indicates increase in mechanical properties by the addition of HNT into the PLA matrix up to 5% loading. The results obtained in this study could be due to the effect of 3D printing parameters which did not increase the mechanical properties. The break point of the tensile test bars as shown in Fig. 3 is mostly near the neck and in line with the infill of the tensile bars which indicates that 3D printing parameters have to be optimized which had significant influence on the mechanical properties.

Fig. 3. Photographs of 3D printed tensile bars after testing (a) PLA (b) PLA/HNT 3% (c) PLA/HNT 5% indicates the breaking point of the bars during testing is influenced by the 3D printing processing.

Thermal properties of the 3D printed nanocomposites were analysed by the method of DSC and the results are as shown in the Fig 4. There is no significant difference in the glass transition temperature (T_g) by the addition of HNT into the PLA matrix. However, the cold crystallisation temperature (T_{cc}) significantly decreases with increase in HNT percentage which indicates the nucleating effect of the HNT with the PLA.

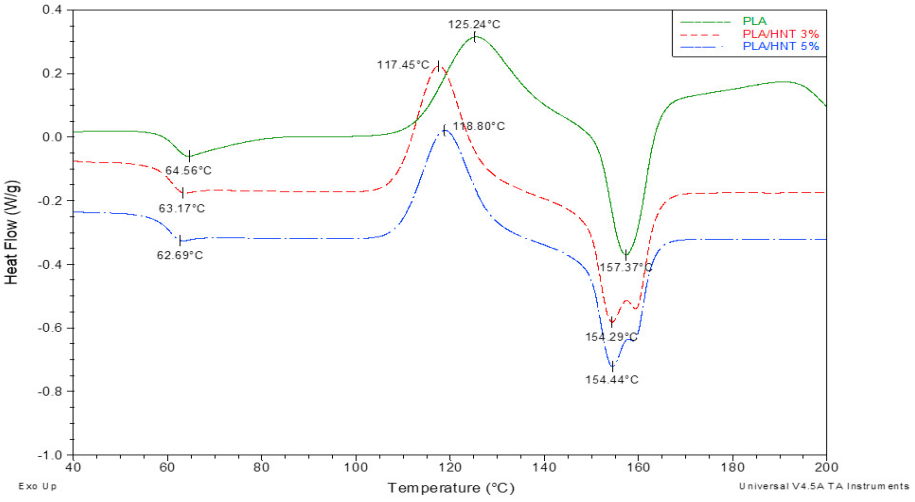

Fig. 4. DSC thermographs of PLA, PLA/HNT 3% and PLA/HNT 5% nanocomposites.

The filaments were 3D printed as 25 mm medical implants as shown in Fig 5. The printing of the implants for PLA filament was easy when compared to the nanocomposites. However, all the stents had rough finishing as seen in the optical microscope images in Fig 6. which could be due to the nozzle speed between the points. In addition, the 3D printed stents for nanocomposites had bubble like structures at some points which could be due to the influence of percentage of clay along with the processing temperatures.

a b c

Fig. 5. 3D printed implants of (a) PLA, (b) PLA/HNT 3% and (c) PLA/HNT 5% nanocomposites

a b c

Fig. 6. Photographs from optical microscope of 3D printed implants of (a) PLA, (b) PLA/HNT 3% and (c) PLA/HNT 5% nanocomposites

4. Discussion

This research work outlines the possibility of firstly developing nanocomposite filament using biodegradable thermoplastic polymer PLA and nanoclay HNT. This developed PLA/HNT nanocomposite filament could further be 3D printed by the method of FFF into standard tensile test bars and model medical implants. The printability, morphology, thermal and mechanical properties were evaluated. Analysis showed that the ease of printing and the morphology of the printed tensile bars and implants varied with the clay compositions as the printing parameters were maintained the same for all the PLA and PLA/HNT nanocomposite batches for comparison.

Ease of maintenance, low cost and flexibility make the FFF the most commonly preferred process of 3D printing [9]. However, some disadvantages such as surface roughness, need for support material and support removal and mainly imperfect sealing between layers and toolpaths [5] have to be considered while FFF process. In this study as

the printing parameters were same for all the batches, the mechanical properties of the 3D printed tensile bars were not in correlation with the mechanical properties of the PLA/HNT nanocomposite. As illustrated in Fig. 3, the breaking point of the tensile bars was mostly at the neck and in line with the printing pattern of the bars. This suggests that delamination between layer occurred. This effect can be reduced by adjusting the 3D printing parameters such as infill pattern, temperature and nozzle speed. Similar breakage at the neck was shown by the study of mechanical properties by the influence of FFF printing parameters by Kalinowski et. al. Minor discontinuities in filament extrusion, uncontrolled shrink during the cooling process, weakness between the layers could lead to the decrease in the mechanical properties of the 3D printed parts [15]. It is also reported that FFF reduces the properties of the 3D printed parts as may create void spaces between the material deposition lines [16].

However, thermal analysis of the 3D printed PLA/HNT nanocomposites is in correlation with the thermal analysis of the PLA/HNT as a nanocomposite. Thermal analysis suggest a significant decrease in cold crystallisation temperature and negligible decrease in melting temperature. The glass transition temperature T_g is a measure of rigidity [17]. There is no significant difference in the glass transition temperature. However, the decrease in the cold crystallisation temperature indicated that nanocomposites are more likely crystallized which could be due to the nucleating effect of HNTs on the PLA [18], [19] and that heterogeneous nucleation was likely to occur where thinner crystalline lamella was formed compared to that of virgin PLA [20]. Hence the melting temperature of the composite is also lower than that of virgin PLA. Based on the above result, the composite appears to have an amorphous (low crystalline) structure. HNTs acting as the nucleating agent in the PLA crystallises the PLA/HNT composite more quickly than the virgin PLA [18], [19], [21].

During the 3D printing process, the nozzle movement in X-Y direction induces uniform heat transfer allowing crystallization [11]. However, in our study the results differ, which could be due to the nucleating effect of HNT on the PLA matrix decreasing the cold crystallisation temperature. Similar results are obtained in the study of CNT-Graphene based polymer nanocomposite for 3D printing by FFF [11].

3D printed implants were successfully fabricated into mesh forms using FFF's layer-by-layer approach composed of PLA/HNT nanocomposite.

4. Conclusion

In this study, it was possible to develop 3D printing filament using biodegradable PLA and reinforcing with biocompatible filler HNT. The filament had a diameter 1.75±0.10 mm for use in FFF 3D printing. The 3D printed model implants were successfully fabricated into mesh forms whose mechanical properties can be enhanced by optimizing the printing parameters. In future work, the other properties of the nanocomposites such as melt flow and viscosity will be further investigated in order to optimize printing parameters for higher mechanical properties and good finishing of the 3D printed model implants.

Acknowledgements

This work was supported in part by financial support from Athlone Institute of Technology under the Presidents Seed Fund, Enterprise Ireland funding under the Technology Gateway program, grant number TG-2017-0114 and Science Foundation Ireland (SFI) under Grant Number 16/RC/3918, co-funded by the European Regional Development Fund.

References

[1] G. M. Paul et al., "Medical Applications for 3D Printing: Recent Developments." Mo. Med., vol. 115, no. 1, pp. 75–81, 2018.

[2] A. J. Guerra, P. Cano, M. Rabionet, T. Puig, and J. Ciurana, "3D-printed PCL/PLA composite stents: Towards a new solution to cardiovascular problems," Materials (Basel)., vol. 11, no. 9, pp. 1–13, 2018.

[3] R. F. Youssef et al., "Applications of three-dimensional printing technology in urological practice," BJU Int., vol. 116, no. 5, pp. 697–702, 2015.

[4] D. Mills, K. Tappa, U. Jammalamadaka, J. Weisman, and J. Woerner, "The Use of 3D Printing in the Fabrication of Nasal Stents," Inventions, vol. 3, no. 1, p. 1, 2017.

[5] D. Pranzo, P. Larizza, D. Filippini, and G. Percoco, “Extrusion-Based 3D Printing of Microfluidic Devices for Chemical and Biomedical Applications: A Topical Review,” Micromachines, vol. 9, no. 8, p. 374, 2018.
[6] C. Miguel, C. Estomba, I. González Fernández, M. Ángel, and I. Otero, “3D Printing for Biomedical Applications: Where Are We Now?,” Eur. Med. J., vol. 2, no. 1, pp. 16–22, 2017.
[7] E. Fuenmayor et al., “Material considerations for fused-filament fabrication of solid dosage forms,” Pharmaceutics, vol. 10, no. 2, pp. 1–27, 2018.
[8] P. Lamberti et al., “Evaluation of thermal and electrical conductivity of carbon-based PLA nanocomposites for 3D printing,” vol. 020158, p. 020158, 2018.
[9] S. Berretta, R. Davies, Y. T. Shyng, Y. Wang, and O. Ghita, “Fused Deposition Modelling of high temperature polymers: Exploring CNT PEEK composites,” Polym. Test., vol. 63, pp. 251–262, 2017.
[10] B. Coppola, N. Cappetti, L. Di Maio, P. Scarfato, and L. Incarnato, “3D printing of PLA/clay nanocomposites: Influence of printing temperature on printed samples properties,” Materials (Basel)., vol. 11, no. 10, pp. 1–17, 2018.
[11] K. Gnanasekaran et al., “3D printing of CNT- and graphene-based conductive polymer nanocomposites by fused deposition modeling,” Appl. Mater. Today, vol. 9, pp. 21–28, 2017.
[12] T. D. Ngo, A. Kashani, G. Imbalzano, K. T. Q. Nguyen, and D. Hui, “Additive manufacturing (3D printing): A review of materials , methods , applications and challenges,” Compos. Part B, vol. 143, no. December 2017, pp. 172–196, 2018.
[13] R. Dermanaki Farahani and M. Dubé, “Printing Polymer Nanocomposites and Composites in Three Dimensions,” Adv. Eng. Mater., vol. 1700539, pp. 1–9, 2017.
[14] O. Ivanova, C. Williams, and T. Campbell, “Additive manufacturing (AM) and nanotechnology: promises and challenges,” Rapid Prototyp. J., vol. 19, no. 5, pp. 353–364, 2013.
[15] G. Ćwikła, C. Grabowik, K. Kalinowski, I. Paprocka, and P. Ociepka, “The influence of printing parameters on selected mechanical properties of FDM/FFF 3D-printed parts,” IOP Conf. Ser. Mater. Sci. Eng., vol. 227, no. 1, 2017.
[16] R. T. L. Ferreira, I. C. Amatte, T. A. Dutra, and D. Bürger, “Experimental characterization and micrography of 3D printed PLA and PLA reinforced with short carbon fibers,” Compos. Part B Eng., vol. 124, pp. 88–100, 2017.
[17] D. M. Devine, E. Hoctor, J. S. Hayes, E. Sheehan, and C. H. Evans, “Extended release of proteins following encapsulation in hydroxyapatite/chitosan composite scaffolds for bone tissue engineering applications,” Mater. Sci. Eng. C, vol. 84, no. November 2016, pp. 281–289, 2017.
[18] W. Wu, X. Cao, Y. Zhang, and G. He, “Polylactide/halloysite nanotube nanocomposites: Thermal, mechanical properties, and foam processing,” J. Appl. Polym. Sci., vol. 130, no. 1, pp. 443–452, 2013.
[19] M. Liu, Y. Zhang, and C. Zhou, “Nanocomposites of halloysite and polylactide,” Appl. Clay Sci., vol. 75–76, pp. 52–59, 2013.
[20] Y. Dong et al., “Polylactic acid (PLA)/halloysite nanotube (HNT) composite mats: Influence of HNT content and modification,” Compos. Part A Appl. Sci. Manuf., 2015.
[21] Y. Chen, A. Murphy, D. Scholz, L. M. Geever, J. G. Lyons, and D. M. Devine, “Surface-modified halloysite nanotubes reinforced poly(lactic acid) for use in biodegradable coronary stents,” J. Appl. Polym. Sci., vol. 135, no. 30, p. 46521, Aug. 2018.